Tutor/s

Dr. Joan Formosa Mitjans
Departament de Ciència dels Materials i Enginyeria Metal·lúrgica

Sr. Sergio Huete Hernández
Departament de Ciència dels Materials i Enginyeria Metal·lúrgica

UNIVERSITAT DE BARCELONA

Grau d'Enginyeria de Materials

Treball Final de Grau

Design of a Lab-scale system for the study of dry desulfurization process.

Disseny d'un sistema a escala laboratori per a l'estudi de dessulfuració per via seca.

Raúl Gil Sáenz

June 2018

UNIVERSITAT DE BARCELONA

Dos campus d'excel·lència internacional

B:KC Barcelona Knowledge Campus

HUB Health Universitat de Barcelona Campus

Intelligence is the ability to adapt to change

Stephen Hawking

En primer lugar**,** me gustaría agradecer al grupo de investigación DIOPMA la confianza depositada en mí para la realización de este proyecto. Especialmente a mis tutores, Joan Formosa Mitjans y Sergio Huete Hernández, que desde el primer momento me han apoyado y aconsejado para afrontar este trabajo.

También me gustaría agradecer el consejo y ayuda de los doctores Ricard Torres Castillo, Esther Chamarro Aguilera y muy especialmente al Dr. Joan Llorens Llacuna del departamento de Ingeniería Química y Química Analítica de la Universidad de Barcelona sin el cual hubiera sido muy difícil afrontar algunas áreas de conocimiento que este proyecto requiere.

A todas las personas que he conocido durante estos años en la facultad y que me han brindado su amistad y compañerismo. He aprendido mucho en el día a día y ha sido un placer compartir esta etapa de mi vida con todos ellos.

A mis padres, por su ejemplo, ayuda y sacrificio constante durante todos estos años para que alcance mis objetivos. Gracias a los valores que me habéis inculcado me siento preparado para afrontar nuevos retos tanto a nivel personal como profesional.

REPORT

CONTENTS

1. GLOSSARY

BAT: Best Available Techniques

CAA: Clean Air Amendment

CCM: Caustic Calcined Magnesite

CD: Cyclone Dust

DBM: Dead Burned Magnesite

D-FGD: Dry Flue Gas Desulfurization

DIOPMA: Centro de Diseño y Optimitzación de Procesos y Materiales

EID: Emissions Industrial Directive

FGD: Flue Gas Desulfurization

LG-D: Low Grade Dolomite

LG-F: Low Grade and Fine

LG-MgO: Low Grade Magnesium Oxide

MAGNA: Magnesitas Navarras S.A.

PC8: Low Grade Magnesium Oxide by-product

W-FGD: Wet Flue Gas Desulfurization

2. SUMMARY

Sulphur dioxide (SO_2) is a major contributor to contamination and environmental degradation. The limit emission values are becoming tighter and nowadays, the Industrial Emissions Directive (EID) of the European Union has been demanding the cement, lime, and magnesium oxide industries to reduce their SO_2 emissions by means of sustainable methods.

The main industrial activity of Magnesitas Navarras S.A. (MAGNA), Company located in Zubiri (Navarra, Spain), is obtaining magnesium oxide, MgO, from calcination of natural magnesite $MgCO_3$. Emissions of SO_X are mainly in the form of sulfur dioxide (SO_2), whose emission concentration directly depend on the amount of sulphur contained in the raw material and more importantly in the type of fuel used during the firing process. The reuse of by-products like Low Grade Magnesium Oxide (LG-MgO) during the calcination of magnesite for flue gas desulfurization (FGD) can generate a loop process optimizing the efficiency and revaluating those by-products.

FGD is the widest applied measure for SO_2 reduction. It allows an industrial plant to reduce its emission by up to 99%. Essentially, is an acid-base reaction in wet or dry conditions. Although wet methods present many advantages such as their high desulfurization efficiency and low economic cost, the conclusions also brought up the fact that the large amounts of liquid effluents produced at the end of the process require a proper management.

After research work in wet conditions, MAGNA requested DIOPMA to start a study of Dry FGD. The first benefit of using the dry method is wastes, which are easier to handle than wet flue gas desulfurization. Moreover, requires less energy inputs and lower operation costs. The scope of this project is the lab-scale design to achieve the study of the LG-MgO performance as a desulfurization agent.

There are different considerations to take into account for the design of the lab-scale experiment for the dry desulfurization process: gas composition, flow rate, heat flow, corrosion resistance, among others, in order to achieve the company conditions for a reliable study.

The process of heat exchange becomes the core of the project since the bottles with the gas composition and the particulate solid have been provided by the company. The design requires heating the gas from room temperature to 200ºC before putting it in contact with the LG-MgO. The calculation to determine the fluid flow conditions has been made in order to use the best correlations to approximate the heat transfer system for the project.

The laboratory system designed includes a 1m length furnace and a pipe that goes through to reach the working temperature. Additionally the minimum radius of insulation has been calculated to avoid the heat losses between the exit of the furnace and the the reactor input.

Boundary conditions of energy-efficient walls, for furnace and maximum service temperature or durability for pipe have been studied in order to select the best materials for each one using Granta CES EduPack software.

As a main conclusions for this work, it has been determined that the flow conditions directly influences the convection heat transfer, suggesting a turbulent flow as a better ally for its optimization. On the other hand, another configuration can be made and allows to use a resistance instead of a furnace. Therefore, and an external insulation should be used in order to ensure that all the heat generated is absorbed by the fluid.

3. RESUMEN

El dióxido de azufre (SO_2) es un importante contribuyente a la contaminación y la degradación ambiental. Los valores límite de emisión son cada vez más estrictos y, actualmente, la Directiva de Emisiones Industriales (EID) de la Unión Europea ha exigido a las industrias del cemento, la cal y el óxido de magnesio que reduzcan sus emisiones de SO_2 utilizando métodos sostenibles.

La principal actividad industrial de Magnesitas Navarras S.A. (MAGNA), empresa ubicada en Zubiri (Navarra, España), es la obtención de óxido de magnesio, MgO, a partir de la calcinación de magnesita natural $MgCO_3$. Las emisiones de SO_X son principalmente en forma de dióxido de azufre (SO_2), cuya concentración depende directamente de la cantidad de azufre contenido en la materia prima y, más importante, del tipo de combustible utilizado durante el proceso de calcinación. La reutilización de subproductos como el óxido de magnesio de baja ley (LG-MgO) para la desulfuración de los gases de combustión (FGD) puede generar un proceso en bucle que optimiza la eficiencia del proceso y a la vez revaloriza estos subproductos.

FGD es el tratamiento más aplicado para la reducción de emisiones de SO_2. Permite a una planta industrial reducir su emisión hasta en un 99%. Básicamente, es una reacción ácido-base en condiciones húmedas o secas. Aunque los métodos húmedos presentan muchas ventajas, como su alta eficiencia de desulfuración y su bajo coste económico, su aplicación requiere un manejo adecuado de grandes cantidades de efluentes líquidos producidos al final del proceso.

Tras realizar un trabajo de investigación en condiciones húmedas, MAGNA solicitó al centro DIOPMA comenzar un estudio de FGD en vía seca. Uno de los beneficios del uso del método en seco son los residuos ya que son más fáciles de gestionar que en la desulfuración húmeda. Además, requiere menos energía y menores costes de

operación. El objetivo de este proyecto es el diseño, a escala laboratorio, de un sistema que permita elaborar un estudio del rendimiento del LG-MgO como agente de desulfuración.

Existen diferentes consideraciones a tener en cuenta para el diseño del experimento del proceso de desulfuración seca a escala laboratorio: composición del gas, caudal, flujo de calor, resistencia a la corrosión, entre otros, con el fin de reproducir las condiciones de la planta de forma fidedigna.

El proceso de intercambio de calor se convierte en el núcleo del proyecto debido a que las botellas con la composición del gas y el sólido ya han sido proporcionados por la empresa. El diseño requiere calentar el gas desde temperatura ambiente hasta 200ºC antes de ponerlo en contacto con el LG-MgO. El cálculo para determinar el régimen de flujo del fluido se ha realizado con el fin de utilizar las mejores correlaciones para la determinación de los parámetros de transferencia de calor en el sistema.

El sistema de laboratorio diseñado incluye un horno de 1 m de longitud para calentar la tubería que transporta el fluido hasta alcanzar la temperatura de trabajo. Adicionalmente, se ha calculado el radio mínimo de aislamiento para evitar las pérdidas de calor entre la salida del horno y la entrada del reactor.

Se han estudiado las condiciones de contorno como la optimización de las paredes del horno o la máxima temperatura de servicio y durabilidad de la tubería, con el objetivo de seleccionar los mejores materiales para cada uno mediante el software de Granta CES EduPack.

Como principales conclusiones para este trabajo, se ha determinado que el régimen de circulación influye directamente en la transferencia de calor, sugiriendo un flujo turbulento como un mejor aliado para su optimización. Por otro lado, se puede utilizar otra configuración que permite usar una resistencia en substitución del horno u un aislamiento externo que asegure que todo el calor generado sea absorbido por el fluido.

4. PREFACE

In 2015 a PhD Thesis about reuse of MgO by-products for wet flue gas desulfurization was published [1]. The reuse of natural magnesite calcination by-products it's a sustainable desulfurization method and allows the company to create a loop process revaluing its by-product. Nowadays, another research work has been requested in order to study the viability of dry flue gas desulfurization process. The aim of this project is design the lab-scale installation and conditions to obtain a reliable and representative upcoming study.

4.1. PROJECT ORIGIN

The SO_2 emissions limit imposed by the regional legislation have been continuously reduced due to contribution to contamination and environment degradation. In the last years, Magnesitas Navarras S.A. have requested DIOPMA the study of sustainable methods for reuse its by-products as desulfurization agents to remove the SO_2 of the exhaust calcination gases. The wet desulfurization technique produces wastes and effluents that requires proper management and involves additional costs. The dry desulfurization method could improve these drawbacks enhancing the process efficiency.

4.2. MOTIVATION

The motivation of the present work is design a lab-scale system for the study of the dry desulfurization process by applying the knowledge acquired in various subjects of the Materials Engineering Bachelor's Degree combining them with the prior achieved in Chemical Engineering as heat transfer or fluid mechanics.

5. INTRODUCTION

DIOPMA (Centro de Diseño y Optimitzación de Procesos y Materiales) and MAGNA (Magnesitas Navarras, S.A.) started a collaborative relationship in late 90's. Since then, multiple research works has been undertaken. The collaboration projects have been aimed at developing different routes for reusing and revalorizing the by-products obtained during its industrial activity. As a result, more than 20 research articles have been published in highly recognized international journals along with four patents. The research has covered four different fields of applications:

- Environmental
- Industrial
- Construction
- Renewable energy

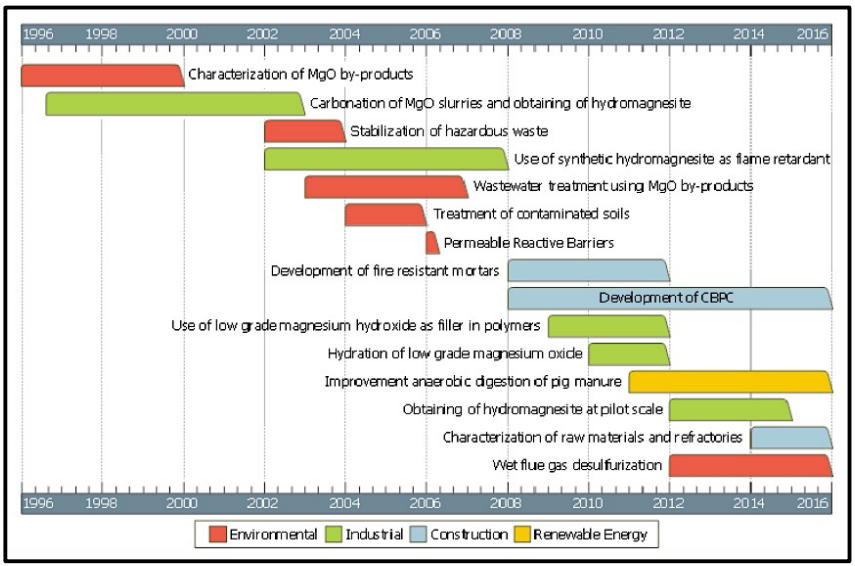

Figure 1. Timeline DIOPMA-MAGNA collaborations [1]

The present work it's addressed to study the design of lab-scale system with the aim of simulate the gas exit conditions of the industrial magnesite calcination process in the company for study the viability of a dry desulfurization process. Before that, the next sections are introduced to put in context the scope of the project.

5.1. SO_2 EMISSIONS

Sulphur dioxide (SO_2) is a major contributor to contamination and environmental degradation. Its removal has been the focus of many researches since the late of the 19th century. Together with the industrial development and the awareness of its negative effects, the need of imposing SO_2 controls began in 1929 in the United Kingdom. The first emission control directive on an EU level was imposed in 1984 and since then many directives have been renewed until the current Industrial Emissions Directive of 2010 and the Best Available Techniques (BAT) reference document of 2013. In the United States the first action of the government occurred on 1955 but it was not until the Acid Rain SO_2 Reduction Program of the 1990 Clean Air Amendment (CAA) program that remarkable and demonstrable results were produced. Among the techniques for reducing SO_2 emissions, flue gas desulfurization (FGD) methods are the most used technology.

The thermal decomposition of $MgCO_3$ generates carbon dioxide (CO_2) and to a lesser extent carbon monoxide (CO). Other significant emissions to air arise from the firing process itself, such as the dust from the particles attrition and the nitrogen oxides (NO_X), divided in the form of nitric oxide (NO) and nitrogen dioxide (NO_2). Emissions of SO_X are mainly in the form of sulphur dioxide (SO_2), whose emission concentration directly depend on the amount of sulphur contained in the raw material (e.g. natural magnesite or briquettes) and more importantly in the type of fuel used during the firing process [2].

The concentrations of SO_2 emissions from the industrial process of the company have been historically close to 4000 $mg \cdot Nm^{-3}$. According to the information provided, in order to comply with the regulatory emission limit of 1856 $mg \cdot Nm^{-3}$ imposed by the

regional legislation (Comunidad Floral de Navarra), the company had to heavily invest in a SO_2 removal process that could lower emissions down to 1800 $mg \cdot Nm^{-3}$.

Sulphuric acid formation in the atmosphere, commonly known as acid rain, it's a serie of photochemical or catalytic reactions [3] derived from SO_2 emissions. SO_2 is oxidized to SO_3 before being hydrated by air humidity:

$$SO_2 + OH^- \rightarrow HSO_3 \quad (1)$$

$$HSO_3 + O_2 \rightarrow HO_2 + SO_3 \quad (2)$$

$$SO_3 + H_2O \rightarrow H_2O - SO_3 \quad (3)$$

$$H_2O - SO_3 \rightarrow H_2SO_4 \quad (4)$$

The negative effects of acid rain are both to human health and environment.

Table 1. Acid rain effects

Human Health	**Environment**
Irritation of eyes, nose and throat	Wildlife in aquatic systems
Breathing difficulties	Acidification of forest soils
Bronco-constriction	Release of toxic metals in lakes

Several legislations started to be introduced when adverse effects began to be known. Since then, limit emission values are becoming tighter with the SO_2. Nowadays, The Industrial Emissions Directive (EID) of the European Union (2010/75/EU) has been demanding the cement, lime, and magnesium oxide industries to reduce their SO_2 emissions to limits as low as 50 $mg\ Nm^{-3}$ by means of sustainable methods.

The lower end of the range is associated with the use of raw materials with low sulphur content and the use of natural gas while the upper end of the range is associated with the use of raw materials with higher sulphur content and/or the use of

sulphur-containing fuels [4].

Actual desulfurization technologies can be divided in three categories:

- Pre-combustion technologies
- Simultaneous combustion of coal and limestone mixtures
- Post-combustion technologies or Flue Gas Desulfurization (FGD)

5.2. CALCINATION OF NATURAL MAGNESITE

The main industrial activity of Magnesitas Navarras S.A. (MAGNA), Company located in Zubiri (Navarra, Spain), is obtaining magnesium oxide, MgO, from calcination of natural magnesite $MgCO_3$. Each year, the company extracts 1,700,000 tons of natural minerals, up to 450,000 tons of magnesium carbonate can be concentrated to obtain a 170,000 tons of MgO.

The minerals classifieds are introduced in two kilns of 80m length at 1100ºC and 1800ºC respectively and the following thermal decomposition reactions occurs:

$$MgCO_{3\,(s)} \rightarrow MgO_{(s)} + CO_{2\,(g)} \quad (5)$$

$$MgCa(CO_3)_{2(s)} \rightarrow MgO_{(s)} + CaO_{(s)} + 2CO_{2(g)} \quad (6)$$

The fuel used is petroleum coke, *petcoke,* injected with primary air and 35% of natural gas. The calcined mineral is tempered, using a double sleeve pipe system with cold water, before being separated in three different particle sizes (< 0.5; 0.5/1 and > 2 mm) to form the following products [5]:

- Dead Burned Magnesite (DBM): obtained at 1800ºC, also known as sintered magnesite is used as refractory in iron & steel industry.
- Caustic Calcined Magnesite (CCM): obtained at 1100ºC, is used in agriculture, livestock, environment and other chemical and industrial applications.

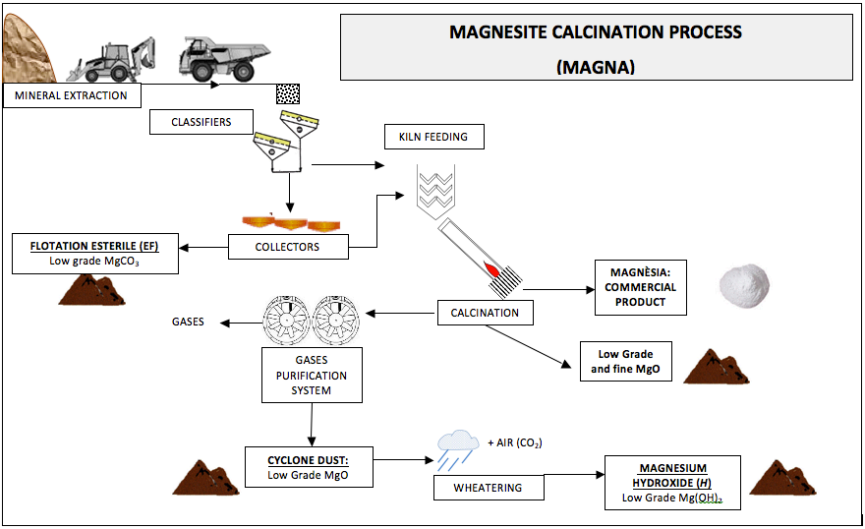

Figure 2. Magnesite calcination process [5]

5.3. MAGNESIUM OXIDE BY-PRODUCTS

During the calcination process many by-products are obtained: Low grade magnesium oxide (LG-MgO), Low grade Dolomite (LG-D), Low grade and fine (LG-F). Essentially these by-products are a mixture with MgO (red line), and dolomite $CaMg(CO_3)_2$ (blue line) as a main compounds [6] which no industry demand. LG-MgO and LG-D are collected as cyclone dust (CD) in the air pollution control (APC) system that treats the combustion gases of the calcination kilns.

These by-products have been studied to evaluate its potential use to alkaline compounds in a FGD [7]. The results showed that the LG-MgO, also named by MAGNA as PC8, had the best SO_2 absorption capability [8].

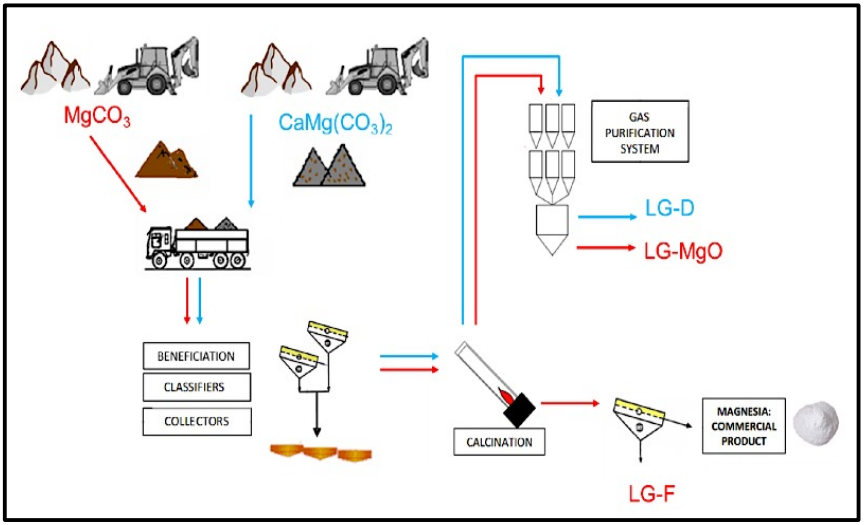

Figure 3. Magnesium oxide by-products [1]

5.4. GENERATING A CLOSING LOOP PROCESS

The company has requested an alternative process apart from the mineral ore extraction, first, increasing the sustainability of the process, and secondly, a valuable commercial product obtained from the revalorization of a by-product. The reuse of by-products during the calcination of magnesite for FGD can generate a loop process optimizing the efficiency and revaluating those by-products (the reaction products can be sold to be used as fertilizers after gas absorption operation system).

Considering the broad experience of the research group, the initial hypothesis in which the research was supported was the potential feasibility of using different types of MgO by-products as desulfurization agents. By this manner, the by-products involved in the emission process itself could be reused in a sustainable and ecological closed loop process.

Moreover, a greater ambition was pursued beyond the demands of the IED and BAT documents: to develop a desulfurization process with 100% removal efficiency, adaptable to the industrial requirements of the company. The use of MgO by-products

with 100% removal efficiency had been never reported in the literature, which supposed a great challenge for the company and the research group from the point of view of novelty contribution to the scientific community.

$$MgO_{(s)} + SO_{2(g)} \rightarrow MgSO_{3(s)}$$

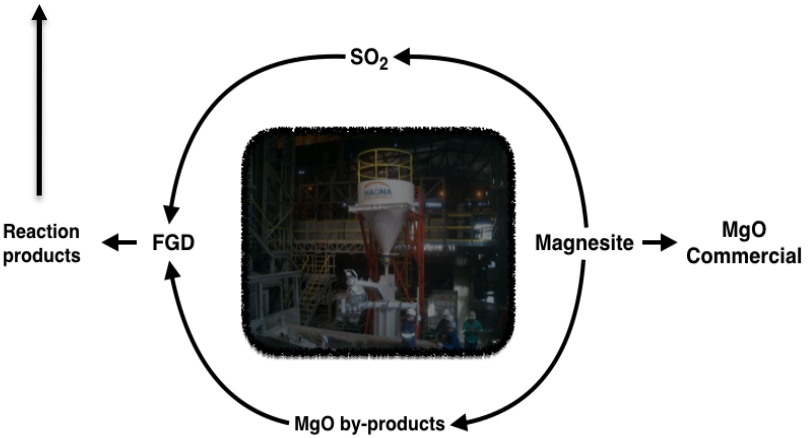

Figure 4. FGD loop process

5.5. FLUE GAS DESULFURIZATION

FGD is the widest applied measure for SO_2 reduction. It allows an industrial plant to reduce its emission by up to 99%. Essentially, FGD is an acid-base reaction between SO_2 (acid) and a dry or wet alkaline solid. FGD technologies also can be classified into the following groups:

- Wet-scrubber technologies
- Spray-dry scrubber technologies
- Dry-scrubber technologies
- Combined SO_2/NO_x removal-process technologies

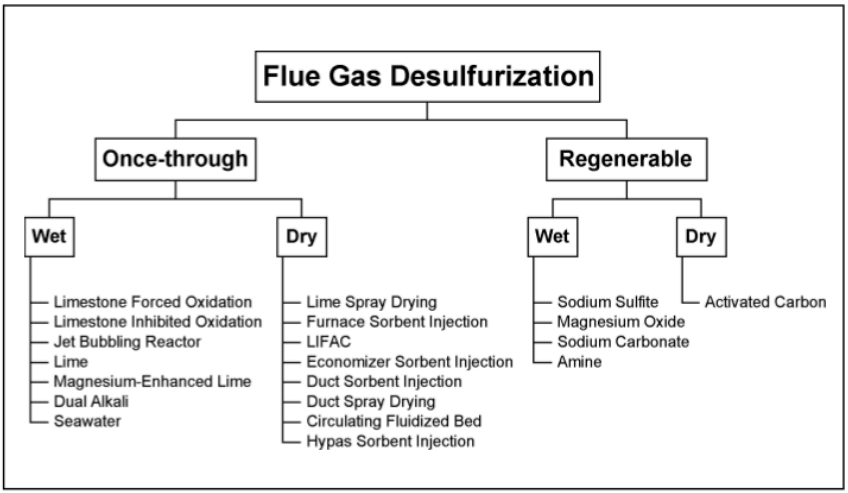

Figure 5. FGD Systems [1]

Wet-scrubber is the most often used method for SO_2 reduction in the energy sector. The market share is about 84% of the total capacity of all desulphurisation methods. The widest applied method among all wet scrubber technologies is wet lime/limestone scrubbers (70% market share).

The estimations of SO_2 emissions reduction costs differ substantially. Even analysing the same technology gives different results. It could be explained as an effect of a specific situation: technical or economic conditions, power-plant localisation, age of power plant, and, what is understandable, interest rate assumed for investment calculation purposes. Therefore, the information about capital and operating costs presented in publications usually cannot be directly transformed for the domestic purposes.

FGD units are absorption scrubbers that are attached to the end of the combustion process of boilers where the combustion flue gas is scrubbed with an alkaline component. FGD systems can operate in wet or dry conditions; wet FGD (W-FGD) technologies have been predominantly selected over the dry type because of their multiple advantages, e.g. high desulfurization efficiency and stable operation, among

others. The contact method between the gas and the alkaline scrubbing agent is based on the nature of the process, which takes place in three stages: diffusion of the solute gas in the film, chemical reaction, and dissolution of the solids.

Nowadays the magnesium-based wet FGD process has been reported to be more suitable for low SO_2 concentration FGD systems because of the low investment required, compact flow sheet and less land occupied, its high efficiency, reliable operation and rare fouling. The absorption process proceeds as follows [9]:

$$MgO + H_2O \rightarrow Mg(OH)_2 \quad (7)$$

$$SO_2 + Mg(OH)_2 + 5H_2O \rightarrow MgSO_3 \cdot 6H_2O \quad (8)$$

$$SO_2 + MgSO_3 \cdot 6H_2O \rightarrow Mg(HSO_3)_2 + 5H_2O \quad (9)$$

$$Mg(HSO_3)_2 + Mg(OH)_2 + 5H_2O \rightarrow 2MgSO_3 \cdot 6H_2O \quad (10)$$

Although wet methods present many advantages such as their high desulfurization efficiency and low economic cost, the conclusions also brought up the fact that the large amounts of liquid effluents produced at the end of the process require a proper management.

5.6. DRY FLUE GAS DESULFURIZATION

Dry-FGD consist on putting dry powdered sorbent in contact with flue gas containing SO_2 [10]. In lime-based sorbents, calcium utilization is limited by the precipitation of calcium sulphite formed on the sorbent surface. These issues can be addressed by modifying the CaO particle characteristics, including the surface area, pore size and distribution, and volume.

Other enhancing approaches include the improvement of the reactivity of the sorbent by blending it with additives, to favour the formation of compounds with a larger specific surface area.

Dry FGD method		Characteristics
LSD	Lime Spray Drying	Rotary atomizers or two-fluid nozzles are used to finely disperse lime slurry into the flue gas.
FSI	Furnace Sorbent Injection	The dry sorbent is injected directly into the section of the furnace where temperature ranges between 950 and 1000°C.
LIFAC	Limestone injected into the furnace with activation of unreacted calcium oxide	It uses limestone as sorbent and removes the waste as a dry solid product in an electrostatic precipitator (ESP). The process involves conventional furnace sorbent injection coupled with an activation reactor that converts unreacted sorbent to hydrated lime for increased SO_2 removal
ESI	Economizer Sorbent Injection	Lime is injected into the convective pass of a coal-fired utility boiler.
DSI	Duct Sorbent Injection	The sorbent is directly injected in the flue gas duct between the air preheater and the particulate control device.
DSD	Duct Spray Drying	The sorbent slurry is sprayed directly into the ductwork upstream the electrostatic precipitator (ESP).
CFB	Circulating Fluidized Bed	The dry sorbent (hydrated lime) is contacted with humidified flue gas in a CFB downstream the air preheater.
HSI	HYPAS (Hybrid pollution abatement system) Sorbent Injection	A dry mixture of lime and recycled solids is injected into the flue gas after particulate removal, cooling and humidification

Figure 6. Dry FGD Methods [1]

The first benefit of use the dry method is wastes, which are easier to dispose than wet flue gas desulfurization [11]. Moreover, requires less energy inputs and lower operation costs. However, the main cons are lower efficiency due to reaction mechanism, magnesium hydroxide, $Mg(OH)_2$, formed in wet method enhances the solid-liquid-gas contact [12]. As with the rest of dry technologies, the conversion of the sorbent and the SO_2 removal efficiency is generally low (50-90%) [13], which has driven the development of many researches over increasing the sorbents reactivity [10] [14].

5.6.1 LG-MgO performance

A sustainable dry desulfurization process was studied by assessing the performance of the by-products obtained during the calcination process of natural magnesite [15]. Thus, the by-products from the calcination process that is producing the SO_2 emissions could be used as desulfurization agents in a closed-loop process. The three by-products under consideration, LG-MgO and LG-D (dust materials from fabric filters) and LG-F

(coarse fraction of the final magnesia product) presented different chemical and physical characteristics. To improve the by-product reactivity toward SO_2, three different HMs were also applied to the raw by-products. Raw LG-MgO (68.1 wt %) presented the best desulfurization potential (litters of SO_2 per kilogram of by-product), up to 25 $L \cdot kg^{-1}$, very convenient compared to the performance of the widely used lime in the same conditions (50 $L \cdot kg^{-1}$). The adsorption capacity of LG-D and LG-F was lower, achieving 16.5 and 15.9 $L \cdot kg^{-1}$, respectively.

5.7. DESIGNING A LAB-SCALE SYSTEM FOR DRY FGD

This chapter is focused on simulating the conditions of dry flue gas desulfurization at laboratory scale. First of all, in the MAGNA plant the contact between the exhaust gases of the chimney and the LG-MgO by-product occurs at approximately 200°C due to the pipes that transport the gas resulting from the calcination to the desulfurization plant.

At the laboratory scale, gas bottles with the composition of the exhaust gases and the particulate solid MgO by-product are available. Therefore, the main objective of the project is to establish adequate operation conditions and materials to enable the contact between the two under the proposed conditions.

There are different considerations to take into account for the design of the lab-scale experiment for the dry desulfurization. Gas composition, flow rate, heat exchange, corrosion resistance, among others. It is remarkable, due to size and availability of the gas bottles, that the flow rate has been setting to 1 $L \cdot min^{-1}$. As discussed above, MAGNA conditions for the contact between gas and particulate solid its around 200ºC, therefore, in the lab-scale system, the pipe has to be heated above this temperature and isolated between furnace exit and reactor input to minimize heat losses.

In the first place, polymeric materials, although they are economical and many of them have a good resistance to many corrosion environments, have been discarded due to the working temperature. In the case of ceramic materials the working temperature does not represent that problem but its fragility and, even more, its porosity

becomes a limiting factor since the fluid is a gas. Metallic materials, in advance, are the selected option in order to approximate and solve the heat transfer equations in the design chapter. In addition, due to the fact that the study will be carried out in a laboratory scale, a 1m length cylindrical furnace has been considered.

5.8. OBJECTIVES

The objectives for the present work are listed as follows:

- Design the laboratory system for an upcoming research works of the dry desulfurization process.

- Establish the theoretical optimal performance for the heat transfer and find the correlations which suits the particular gas flow conditions. In addition, suggest possible solutions to setbacks in order to improve the efficiency and costs.

- Select the best materials for the furnace and gas pipe after analysing the boundary conditions for each one.

- Propose an alternative system to carry out the contact between the gas and the particulate solid for the same proposed conditions.

6. DESIGN

This section is dedicated to explain in detail the system used and evaluate the necessary operation parameters for assessing the heat transfer and flow conditions to achieve the study of the lab-scale dry flue gas desulfurization process.

6.1. EXPERIMENTAL SET-UP

The flow of gas considered for the experiment is 1L·min^{-1} controlled with a flowmeter. The mixture contains the same composition of the MAGNA chimney and it is also provided by the company:

- 78,5% N_2
- 12% CO_2
- 9,5% air
- 0,025% SO_2

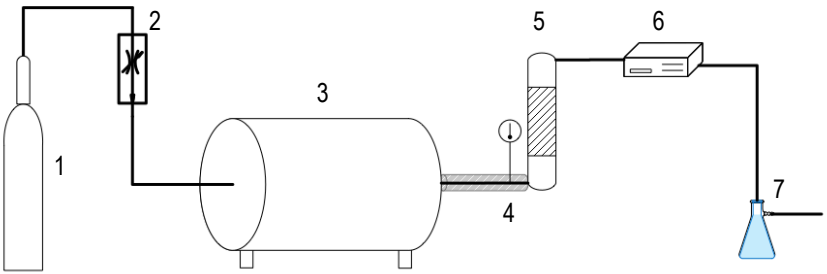

Figure 7. Lab-Scale Set-up

Gas bottle (1) is connected to a flowmeter (2) to adjust the desired flow rate. The tube gas enters in the furnace (3) to rise the work temperature, 200ºC. A Thermometer (4) is placed at the exit to verify exact temperature at the reactor input. Furthermore,

main pipeline must be isolated from the exit of furnace to the reactor entry to decrease the heat losses.

The reactor (5) made of Pyrex glass contains the by-product, LG-MgO, to perform the neutralization of SO_2. The exhausted gas flow at the outlet of the desulfurization reactor is being continuously analysed respect the concentration of SO_2 using an Emerson MLT-1 NGA 2000 gas analyser (6). Finally, exhaust gas is conducted to a scrubber (7) with a NaOH 6M solution.

To simplify the system, the following figures represent the conditions of flow and heat transfer for the proposed conditions. In Figure 9, Tx represents the necessary furnace temperature in order to reach the desired exit gas temperature, and L(x) the necessary pipe length. For the upcoming calculations, a 1m pipe length has been considered.

Figure 8. Simplified flow conditions

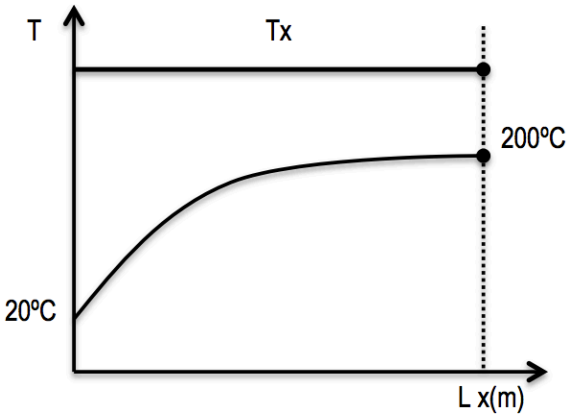

Figure 9. Simplified temperature system

6.2. FLOW CONDITIONS

The flow conditions are directly related to the heat transfer by convection, therefore, it must be previously defined in order to use the suitable equations and correlations for our particular system [16].

In order to characterize the flow movement it is necessary to know the Reynolds number (Re). The Reynolds value is dimensionless and relates the inertial forces against the viscous forces of the fluid, it is widely used in fluid mechanics, reactors design or transport phenomena and its value indicates whether the fluid is in a laminar or turbulent flow [17]. For a fluid that circulates through a straight circular pipe, the Reynolds number is given by [18]:

$$Re = \frac{v \cdot \rho \cdot D}{\mu} \tag{11}$$

Where v is the fluid velocity [m/s], ρ the fluid density [kg/m^3], D, the diameter of the pipe [m] and, μ, the dynamic viscosity [Pa·s].

For Reynolds values $Re \leq 2100$ is considered laminar flow

For Reynolds values $Re \geq 4000$ is considered turbulent flow.

For Reynolds values $2100 \leq Re \leq 4000$ is considered transient flow.

We known the volumetric flow is very low, therefore a smallest pipe diameter (6 mm) has been selected to increase the maximum gas speed inside the pipe:

$$\dot{v} = 1L \cdot min^{-1} \cdot (1m^3/10^3\,L) \cdot (1min/60s) = 1.67 \cdot 10^{-5}\ m^3 \cdot s^{-1}$$

$$D = 6mm = 6 \cdot 10^{-3}\ m$$

$$S = (\pi/4) \cdot D^2 = 2.83 \cdot 10^{-5}\ m^2$$

$$v = \dot{v} / S = 0.59\ m/s$$

For density, viscosity and conductivity, properties that we will need in the following section, the air properties at an average temperature and 1 atm of pressure (for further

information please see Appendix 1) it's a close approximation to estimate the Reynolds number considering the composition of the gas bottle:

Average temperature: Tm = (20 + 200) / 2 = 110 ºC

$\rho = 0.89\ kg/m^3$

$\mu = 2.26 \cdot 10^{-5}\ kg/m \cdot s$

$k = 0.03235\ W/m \cdot K$

$$Re = \frac{v \cdot \rho \cdot D}{\mu} = 139.31$$ Reynolds number clearly indicates a laminar flow

6.3. HEAT TRANSFERENCE

First of all, we must consider that there are two types of heat transmission in the system. On the one hand, forced external convection inside the furnace, between the air and the external pipe wall, conduction through the wall of the pipe that transports the gas and internal convection between the gas and the internal pipe wall. Also, at the exit of the furnace there's also convection that corresponds to the heat losses by contact with the environment prior to entering the reactor. These heat losses should be minimized with the placement of an insulator around the pipe.

For this particular case, we should consider the following equations for the calculation of a global coefficient U that encompasses the two types of heat transfer.

$$\text{Conduction: } q = -k \cdot A \frac{dT}{dx} \quad (12)$$

$$\text{Convection (external): } q = he \cdot A \cdot \Delta T \quad (13)$$

$$\text{Convection (internal): } q = hi \cdot A \cdot \Delta T \quad (14)$$

In general, when heat is transferred between two fluids separated by a solid medium, the use of the individual coefficients relates the heat flow rates with the

temperatures within the fluids and in the separation walls (solid-fluid interface). According to Figure 10, the transmitted heat flux differential will be [16] :

$$dQ = \frac{T-Tw}{\frac{1}{he \cdot dAe}} = \frac{Tw-tw}{\frac{e}{k \cdot dAml}} = \frac{tw-t}{\frac{1}{hi \cdot dAi}} \tag{15}$$

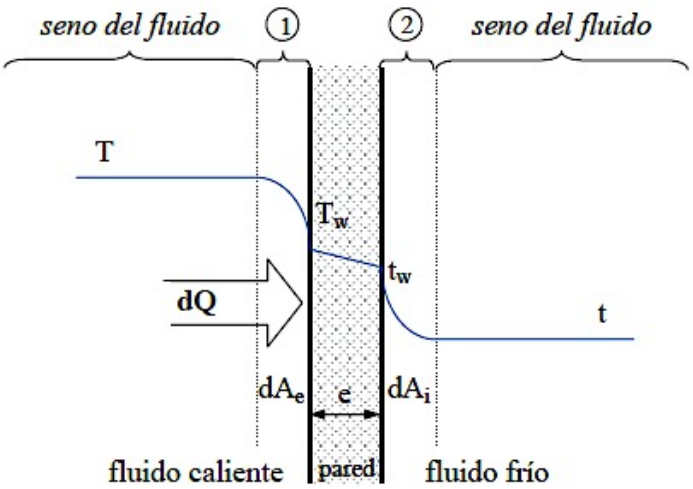

Figure 10. Fluid heat transfer through a solid wall

However, there are particular cases to simplify the previous equation (15):

- If the thickness of the wall is very small:

$$\frac{1}{U} = \frac{1}{he} + \frac{e}{k} + \frac{1}{hi} \tag{16}$$

- if the material of the wall has a high conductivity:

$$\frac{1}{U} = \frac{1}{he} + \frac{1}{hi} \longrightarrow U = \frac{hi \cdot he}{hi+he} \tag{17}$$

The necessary heat transfer to the gas is defined by the following equation:

$$q = \dot{m} \cdot Cp_m \cdot \Delta T \tag{18}$$

Where q is the heat transfer [W], $\dot{m}$, the mass flow [$kg \cdot s^{-1}$], Cp_m the average specific heat capacity [J/kg·K] and ΔT the temperature gradient [K]. The mass flow is the result of the volumetric flow multiplied by the average density of the fluid that is a function of the composition and, therefore, will be very similar to the air:

Table 2. Gas average density

Component	**X_i**	**ρ_i [$kg \cdot m^{-3}$]**
N_2	0.785	1.165
CO_2	0.12	1.842
Air	0.095	1.205
SO_2	0.00025	2.279
$\rho_m = \Sigma (X_i \cdot \rho_i) =$ **1.25 kg · m^{-3}**		

Where X_i represents each component fraction and ρ_i its density. As was predicted before, the average gas density is very close to the air density.

Once obtained, the average density of the fluid we can calculate the mass flow:

$$\dot{v} = 1L/min \cdot (1m^3/10^3\ L)\cdot(1min/60s) = 1.67\cdot10^{-5}\ m^3\cdot s^{-1}$$

$$\dot{m} = 1.67\cdot10^{-5}\ m^3\cdot s^{-1} \cdot 1.25kg \cdot m^{-3} = 2.08 \cdot10^{-5}\ kg\cdot s^{-1}$$

In the same way as the density, the law of mixtures has been used according to the gas composition for the calculation of the average heat capacity of the fluid. Once again, the result reflect the similarity with the air heat specific capacity.

Table 3. Gas average specific heat capacity

Component	Xi	Cp [J/ kg·K]
N_2	0.785	1040
CO_2	0.12	791
Air	0.095	1003
SO_2	0.00025	650
$C\rho_m = \Sigma (X_i \cdot Cp_i) =$ **1007 J / kg·K**		

The gradient of temperatures its also known:

$$\Delta T = T_f - T_0 = (200+273K) – (20+273K) = 180K$$

Finally, we can calculate the heat transfer for the gas with (18):

$$q = \dot{m} \cdot Cp_m \cdot \Delta T = 2{,}08 \cdot 10^{-5}\, kg \cdot s^{-1} \cdot 1007\ J/kg \cdot K \cdot 180K = 3.77 J \cdot s^{-1} = 3.77W$$

For the approach of the problem we should consider the global coefficient of heat transmission U that includes all types of heat transmission present in the system. However, heat conduction transmission can be omitted because metals have a remarkable heat conductivity and the wall thickness of the pipe will be very thin. Therefore the heat transfer can be simplified to Newton's law of cooling:

$$Q = h \cdot A \cdot \Delta T_{ml} \qquad (19)$$

Where h is the convection coefficient [W/m^2K], A is the surface area of the pipe [m^2] and ΔT_{ml} [K] is the logarithmic average temperature gradient that includes a higher temperature value. In our case will be the furnace temperature commented above.

For the calculation of the ΔTml we must assume a value of Tx to be able to calculate the length of pipe necessary inside the furnace, it should also be remembered that the convection coefficient is closely related to the flow regime of the fluid and a turbulent flow enhance the convection and therefore the transmission of heat from the walls to the fluid.

Assuming a furnace stable temperature of 400°C the ΔT_{ml} would be the following:

$$\Delta T_{ml} = \frac{(Tx-Ti)-(Tx-Tf)}{\ln \frac{(Tx-Ti)}{(Tx-Tf)}} = \frac{(400-20)-(400-200)}{\ln \frac{(400-20)}{(400-200)}} = 280{,}44K \quad (20)$$

An interesting case is the circulation in a laminar flow when the temperature of the wall remains constant; situation when a process occurs with high h. In this case, a theoretical study indicates that in the region of profiles of laminar speed and constant heat flux is met [16]. Nusselt number for this case is Nu = 4,3636 and relates the h.

$$Nu = \frac{h \cdot D}{k} \rightarrow h = \frac{Nu \cdot k}{D} = 17.091\ W/m^2 \cdot K \quad (21)$$

Finally, the constant heat flux needed according to the external surface pipe area is defined by:

$$q_w = q / S = q / 2\pi \cdot r \cdot L = 150.01\ W/m^2 \quad (22)$$

Knowing the necessary power for the process and also known the voltage (V = 220V) we can use the ohm law to know the resistance needed for heating the system:

$$V = R \cdot I \rightarrow I = V/R \quad (23)$$

In order to obtain optimal performance and extend the life of the resistance, a factor of 2 is applied to calculate the resistance capacity required for our system:

$$P \cdot 2 = V \cdot I = V \cdot V/R = V^2/R$$

$$R = 220^2/(150.01 \cdot 2) = 161.32\ \Omega$$

Once the resistance value is known, we can calculate the necessary length of the resistance for a given cross section and evaluate it depending on the resistivity of the different materials. Although not very high temperatures are required for our system, in anticipation of future uses that require a higher service temperature, Kanthal® has been considered for made the furnace resistance. Although the relation between diameter and resistance length can be adjusted, for approach the problem a 0,5 mm diameter Kanthal® wire has been considered. The necessary length is given by:

$$R = \rho \frac{l}{S} \quad \rightarrow \quad l = \frac{R \cdot S}{\rho} = \frac{161.32\ \Omega \cdot 1.96 \cdot 10^{-7} m^2}{1.45 \cdot 10^{-6}\ \Omega \cdot m} = 21{,}8m \tag{23}$$

6.4. PIPE INSULATION

Once the gas has obtained the exit temperature, we must insulate the pipeline between exit and reactor input in order to minimize the heat losses by convection. The equation that relates the heat is the same as in the previous section with the difference that now the transfer goes in the opposite direction.

We know that adding more insulation to a wall always decreases heat transfer. The thicker the insulation, the lower the heat transfer rate. This is expected, since the heat transfer area A is constant, and adding insulation always increases the thermal resistance of the wall with- out increasing the convection resistance.

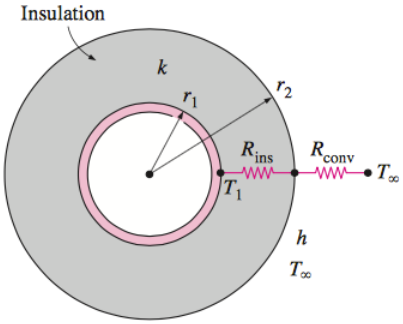

Figure 11. Pipe insulation [17]

Adding insulation to a cylindrical pipe is a different matter. The additional insulation increases the conduction resistance but decreases the convection resistance of the surface because of the increase in the outer surface area for convection. The heat transfer from the pipe may increase or decrease, depending on which effect dominates.

Considering our cylindrical pipe of outer radius r_1, whose outer surface temperature T_1 is maintained constant (Figure 11). The pipe is now insulated with material conductivity is k and outer radius is r_2. Heat is lost from the pipe to the surrounding medium at temperature $T\infty$ with a convection heat transfer coefficient h. The rate of heat transfer from the insulated pipe to the surrounding air can be expressed as:

$$Q = \frac{T_1 - T_\infty}{R_{ins} + R_{conv}} = \frac{T_1 - T_\infty}{\frac{\ln(r_2/r_1)}{2\pi L k} + \frac{1}{h(2\pi r_2 L)}} \tag{24}$$

The variation of Q with the outer radius of the insulation r_2 is represented in (Figure 12) The value of r_2 at which Q reaches a maximum is determined from the requirement that $dQ/dr_2=0$. Performing the differentiation and solving for r_2 yields the critical radius of insulation for a cylindrical body [19]. Considering wood glass (k=0,040 W/K·m^2) as an insulator material for our system, the critical radius is defined by:

$$R_{cr} = \frac{k}{h} = 0.00234 \text{ m} \tag{25}$$

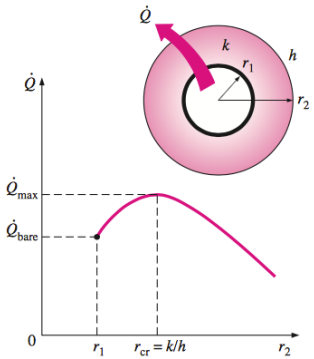

Figure 12. Heat flow vs insulation radius [17]

7. MATERIAL SELECTION

7.1. FURNACE

7.1.1. Preliminary considerations

The energy cost of a furnace is considerable. Part is the cost of the energy which is lost by conduction through the furnace walls; it is reduced by choosing a wall material with a low conductivity, and by making the wall thick. The rest is the cost of the energy used to raise the walls of the furnace and its contents to the operating temperature. It is reduced by choosing a wall material with a low heat capacity, and by making the wall thin. There is a performance index which captures these apparently conflicting design.

Table 4. Energy-efficient furnace walls

Function	Thermal insulation for furnace walls
Objectives	Minimize energy consumed Minimize cost of insulating material
Constraints	Maximum operating temperature (1000K) Possible limit of wall-thickness

The temperature rises from ambient, T_o, to the desired temperature, T. The energy consumed has two contributions. The first is the heat conducted out. Once a steady-state has been reached, the heat loss per unit area by conduction, Q_1, is given by the first law of heat flow [20]:

$$Q_1 = \lambda \frac{dT}{dx} t = \lambda \frac{T\text{-}To}{w} \tag{26}$$

Here λ is the thermal conductivity, dT/dx is the temperature gradient and w is the wall thickness. The second contribution is the heat absorbed by the furnace wall itself. Per unit area, this is:

$$Q_2 = Cp \cdot \rho \cdot w \cdot \left(\frac{To\text{-}T}{2}\right) \tag{27}$$

Where Cp is the specific heat and ρ is the density. The factor 2 enters because the average wall temperature is (T–To)/2. The total energy consumed per unit area of wall is the sum of these two heats:

$$Q = Q_1 + Q_2 = \lambda \frac{T\text{-}To}{w} + Cp \cdot \rho \cdot w \cdot \left(\frac{To\text{-}T}{2}\right) \tag{28}$$

A wall which is too thin loses much energy by conduction, but absorbs little energy in heating the wall itself. One which is too thick does the opposite. There is an optimum thickness, which we find by differentiating equation (28) with respect to wall thickness w:

$$W = \left(\frac{2 \cdot \lambda \cdot t}{Cp \cdot \rho}\right)^{1/2} = (2\alpha t)^{1/2} \tag{29}$$

Where $\alpha = \lambda/Cp \cdot \rho$ is the thermal diffusivity. The quantity $(2\alpha t)^{1/2}$ has dimensions of length and is a measure of the distance heat can diffuse in time t. Equation (29) says that the most energy-efficient furnace wall is one that only starts to get really hot on the outside as the cycle approaches completion. That sounds as if it might lead to a very thick wall, so we must include a limit on wall thickness [21].

Substituting equation (29) back into equation (28) to eliminate w gives:

$$Q = (T\text{-}To)\,(2t)^{1/2}\,(\lambda \cdot Cp \cdot \rho)^{1/2} \tag{30}$$

Q is minimized by choosing a material with a low value of the quantity $(\lambda \cdot Cp \cdot \rho)^{1/2}$, that is, by maximizing:

$$\mathbf{M_1} = (\lambda \cdot Cp \cdot \rho)^{-1/2} = \frac{\alpha^{1/2}}{\lambda} \tag{31}$$

Now the limit on wall thickness. A given time, t, and wall thickness, w, defines, via equation (29), an upper limit for the thermal diffusivity, α:

$$\alpha \leq \frac{w^2}{2t} \tag{32}$$

Selecting materials which maximize equation (31) with the constraint (32) minimizes the energy consumed per cycle. Some candidates for the insulation could be very expensive. We therefore need a second index to optimize on cost.

The cost of the insulation per unit area of wall is:

$$C = C_m \cdot \rho \cdot w \tag{33}$$

Where C_m is the material cost per kg. Substituting for w from equation (29) gives:

$$C = (2t)^{1/2} C_m \left(\frac{\lambda \rho}{Cp}\right)^{1/2} = C_m \rho (2\alpha t)^{1/2} \tag{34}$$

The cost of the material is minimized by maximizing:

$$\mathbf{M_2} = \frac{1}{Cp \cdot \rho} \left(\frac{1}{\alpha}\right)^{1/2} \tag{35}$$

Finally, the material must be able to tolerate an operating temperature of 1000 K.

7.1.2. Selection

The neatest way to approach this problem is by a three-stage selection, starting with a chart of the thermal diffusivity (a compound-property) plotted against thermal conductivity, λ, as in Figure 13. Contours of M_1 are lines of slope 2. One has been positioned at $M_1 = 10^{-3}$. To this can be added lines of constant wall thickness, corresponding to fixed values of thermal diffusivity.

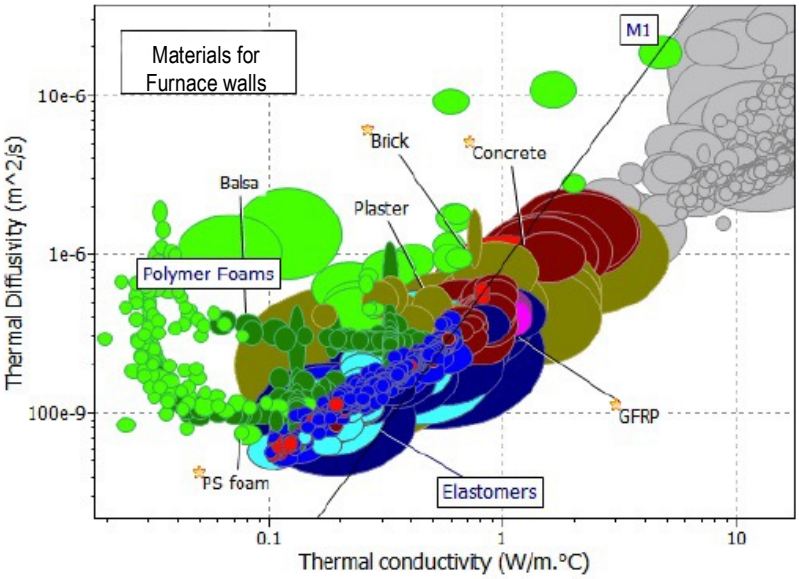

Figure 13. Thermal difussivity vs Thermal conductivity

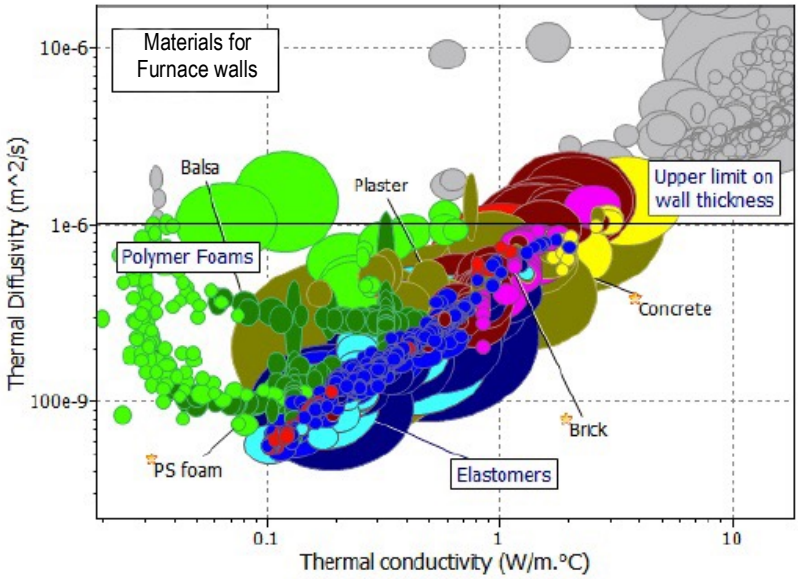

Figure 14. Thermal difussivity vs Thermal conductivity

The right-hand scale shows these limits; the horizontal broken line describes a thickness limit of 200 mm. We can now read-off the best materials for furnace walls to minimize energy, including the limit on wall thickness. Below the broken line, we seek materials which maximize M_1 while meeting the constraint on w.

The second stage optimizes a typical example of the cost of material for given conditions (35). The line shows M2; once again limits on wall thickness can be added (right-hand scale and horizontal line).

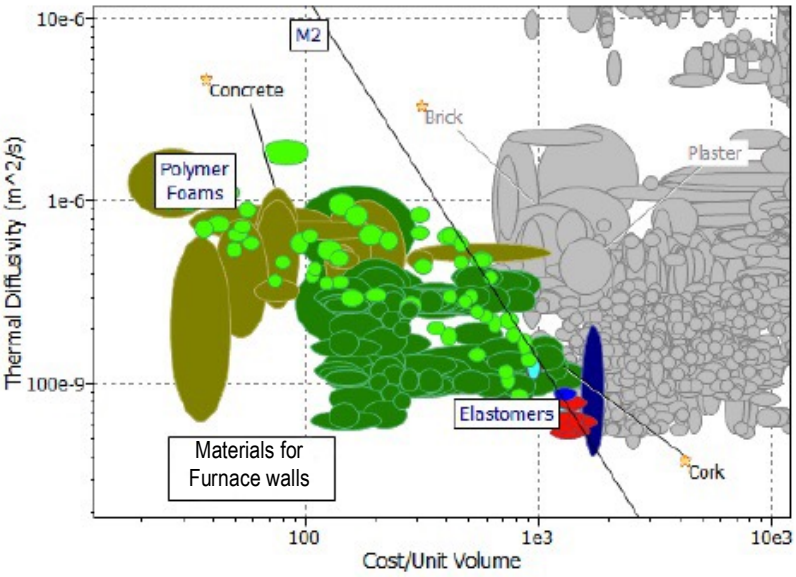

Figure 15. Thermal diffusivity vs Cost / Unit Volume

The selection line of slope -2 shows M2; materials below the line are the best choice, provided they lie within the thickness-limit (right-hand scale and horizontal broken line on figure 16).

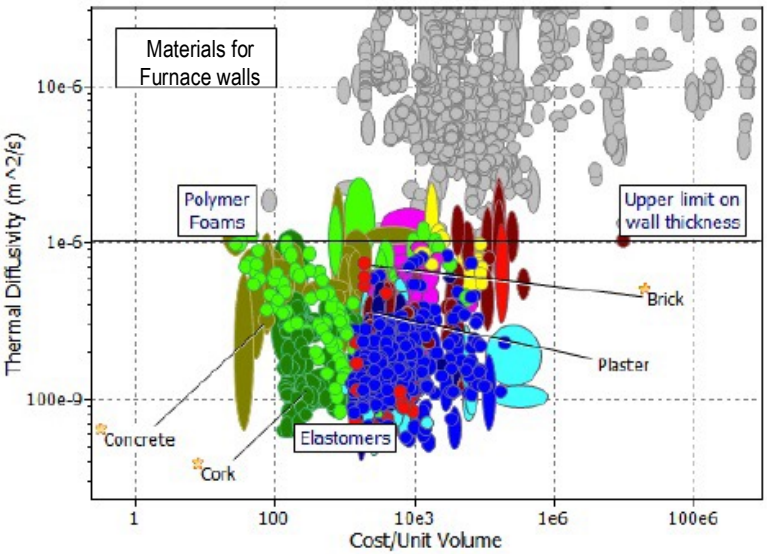

Figure 16. Thermal diffusivity vs Cost / Unit Volume

The final stage is a bar-chart of maximum operating temperature T_{max} > 1000K. The line limits the selection to the region.

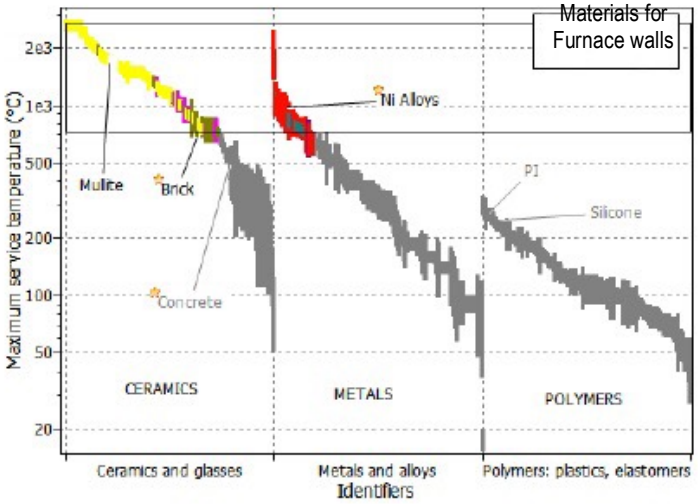

Figure 17. Bar-chart with Tmax > 1000K

Porous ceramics, including firebrick, are the obvious choice but the degree of porosity is important. The more porous, low density, firebricks lie highest under the dashed line on Figure 14, the require the thickest wall. So it may pay to use a dense firebrick to meet the requirements on wall thickness

7.2. PIPE

7.2.1. Preliminary considerations

Pipes can be made of different materials, the choice is usually based on the nature of the fluid circulating inside and its temperature and pressure conditions. Corrosion it's also a problem for most metals, it is related to the fluid composition and usually increases exponentially with temperature.

In our lab-scale system, the SO_2 content, despite being low, can create acid corrosion problems. Particularly, it could form sulfuric acid if it comes into contact with atmospheric vapour. In addition, connections, in the case of being metallic, they must be between metals with very similar potentials to avoid the creation of galvanic cells.

As commented before a metallic pipe has been selected due to conditions of the experiment as a type of fluid or working furnace temperature. As a result, the following selection is focused on metallic materials.

7.2.2. Selection

Corrosion resistance is a complex phenomenon in metals and can not be simplified to be evaluated graphically with Granta CES Edupack software. However, there is the option to apply limits to the selection in terms of resistance to a given environment (for further information see Appendix 2). In our case, excellent resistance to strong acids has been selected. Figure 18 shows the maximum service temperature against the price for materials with excellent durability for strong acids environment.

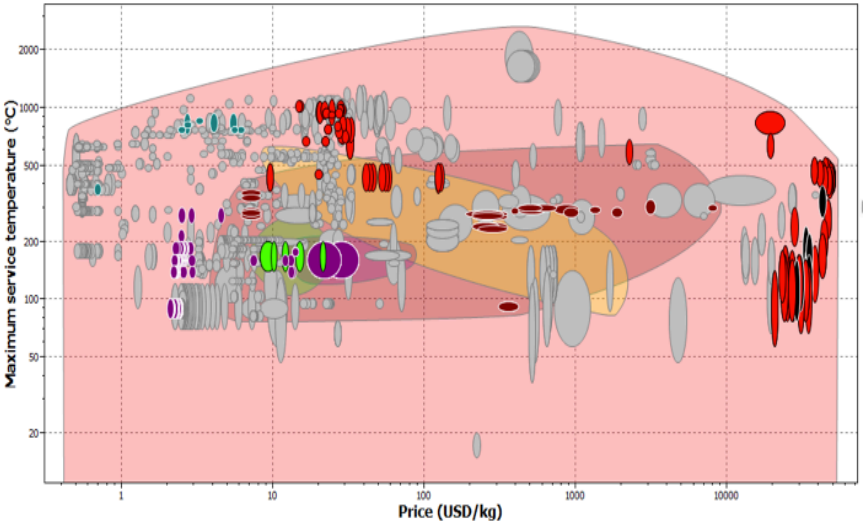

Figure 18. Maximum service temperature vs price

Another important parameter to set is maximum work operating temperature and, although for the calculations a 400ºC for furnace continuous temperature has been considered, its appropriate to establish a higher value to be able to solve possible drawbacks.

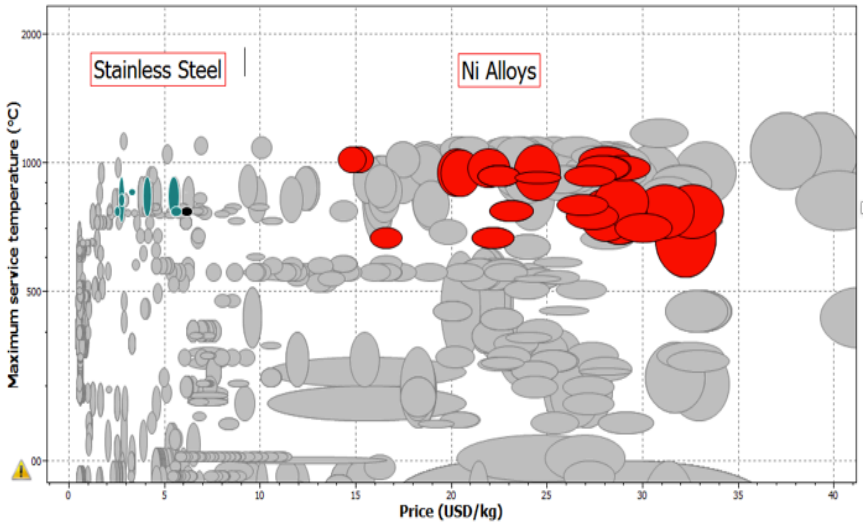

Figure 19. Maximum service temperature vs price

Figure 19, shows the materials that have passed 600ºC minimum value for maximum service temperature.

The results show the stainless steels and Nickel alloys, mainly Inconel®, as the right choice. Both options have a similar maximum service temperature but there is a big gap between its prices. It would be a mistake to finalize the selection in this step since it is necessary to verify that the stainless steels selected, the best choice for the cost, can be provided by the market with the desired pipe characteristics of small diameter and wall thickness.

Fortunately, in the list of materials that meet the requirements, we can find the well-known stainless steels AISI 316, AISI 304, AISI 304L or AISI 316L that are available in multiple diameters and thickness, among them those selected to carry out the calculations for the design section.

8. CONCLUSIONS

The main conclusions for the present work are listed as follows:

The flow mechanics are an essential calculation in order to optimize the heat transfer. An increase in the flow rate, for the same pipe section, would greatly increase the gas velocity in order to achieve turbulent flow. A turbulent regime enhances the convection coefficient and improves the energy efficiency of the process.

The heat flow, temperatures, heat transfer coefficients and parameters has been calculated by theoretical equations, variations in values for all of them should be considered after the system start up. A thermocouple at the reactor input can be connected to the furnace to adjust the working temperature.

The critical insulation radius calculated is the minimum thickness to avoid an increase of heat losses. Therefore, a higher thickness must be used to keep the gas outlet temperature constant.

The chosen method for heat transfer is not unique. Another design can be made without a furnace which consists of a resistance around the pipe and an insulator during the whole conduction. This alternative method allows all the heat generated by the resistance is transferred to the fluid.

Although the low SO_2 concentration, the material selection for the pipe is critical since corrosion can appear and the wall thickness is extremely thin. Stainless steels as AISI 304 or AISI 316 gather the optimal properties to avoid this drawback at the working temperature.

9. REFERENCES AND NOTES

[1] R. del Valle Zermeño, *Flue gas desulfurization processes using by-products from the calcination of magnesite / Ricardo del Valle Zermeño ; directors de la tesi: Josep Maria Chimenos Ribera; Joan Formosa Mitjans*. 2015.

[2] A. Andrews and R. K. Lattanzio, "Petroleum coke: Industry and environmetnal issues," *Congr. Res. Serv.*, p. 29, 2013.

[3] J. A. Phillips and Leopold, "Microwave detection of a key intermediate in the formation of atmospheric sulfuric acid: The structure of H2O-SO3," *J. Phys. Chem.*, vol. 99, no. 2, pp. 501–504, 1995.

[4] E. Parliament and M. States, "Commission Implementing Decision of 26 March 2013 on establishing the best available techniques (BAT) conclusions under Directive 2010/75/EU of the European Parliament and of the Council on industrial emissions for the production of cement, lime and magne," no. 6, pp. 1–45, 2013.

[5] J. Formosa Mitjans, "Formulaciones de nuevos morteros y cementos especiales basadas en suproductos de magnesio," *TDX (Tesis Dr. en Xarxa)*, Dec. 2012.

[6] R. del Valle-Zermeño, J. Giro-Paloma, J. Formosa, and J. M. Chimenos, "Low-grade magnesium oxide by-products for environmental solutions: Characterization and geochemical performance," *J. Geochemical Explor.*, 2015.

[7] R. Del Valle-Zermeño, "Flue Gas Desulfurization Processes using By-products from the Calcination of Magnesite," 2015.

[8] R. Del Valle-Zermeño, J. De Montiano-Redondo, J. Formosa, J. M. Chimenos, M. J. Renedo, and J. Fernández, "Reutilization of MgO byproducts from the calcination of natural magnesite in dry desulfurization: A closed-loop process," *Energy and Fuels*, 2015.

[9] H. Chen, "Thermogravimetric kinetics of MgSO3·6H2O byproduct from magnesia wet flue gas desulfurization," *Energy and Fuels*, vol. 23, no. 5, p. 2552, 2009.

[10] J. Fernández and M. J. Renedo, "Study of the influence of calcium sulfate on fly ash/Ca(OH)2 sorbents for flue gas desulfurization," *Energy and Fuels*, 2003.

[11] "SO2 scrubbing technologies: A review - Srivastava - 2001 - Environmental Progress - Wiley Online Lib."

[12] R. del Valle-Zermeño, J. M. Chimenos, J. Formosa, and A. I. Fernández, "Hydration of a low-grade magnesium oxide. Lab-scale study," *J. Chem. Technol. Biotechnol.*, vol. 87, no. 12, pp. 1702–1708, 2012.

[13] G. Xu, Q. Guo, T. Kaneko, and K. Katou, "A new semi-dry desulfurization process using a powder-particle spouted bed," *Adv. Environ. Res.*, vol. 4, pp. 9–18, 2000.

[14] D. O. Ogenga, M. M. Mbarawa, K. T. Lee, A. R. Mohamed, and I. Dahlan, "Sulphur dioxide removal using South African limestone/siliceous materials," *Fuel*, 2010.

[15] R. Del Valle-Zermeño, J. De Montiano-Redondo, J. Formosa, J. M. Chimenos, M. J. Renedo, and J. Fernández, "Reutilization of MgO byproducts from the calcination of natural magnesite in dry desulfurization: A closed-loop process," *Energy and Fuels*, vol. 29, no. 6, pp. 3845–3854, 2015.

[16] S. Esplugas Vidal and M. E. Chamarro Aguilera, Fundamentos de transmisión de calor. Barcelona : Publicacions i edicions de la Universitat de Barcelona, 2005.

[17] J. M. Cimbala and Y. a. Cengel, "Mecánica de Fluidos: Fundamentos y Aplicaciones" McGrawHill, vol. Primera Ed, pp. 10–11, 2001.

[18] O. Levenspiel, Flujo de fluidos e intercambio de calor. México D. F. : Reverté, 1993.

[19] F. P. Incropera and F. P. Incropera, Fundamentals of heat and mass transfer. Hoboken, NJ [etc.] : John Wiley, 2007.

[20] J. P. Holman, Transferencia de calor, vol. 7, no. 11. 1998.

[21] Ashby, M. F. (2005). Materials selection in mechanical design. Amsterdam: Butterworth-Heinemann.

CES EduPack 2017. Cambridge: Granta Design Limited

APPENDICES

APPENDIX 1: AIR PROPERTIES (1 ATM)

Propiedades del aire a 1 atm de presión

Temp. T, °C	Densidad ρ, kg/m³	Calor específico c_p J/kg · K	Conductividad térmica k, W/m · K	Difusividad térmica α, m²/s	Viscosidad dinámica μ, kg/m · s	Viscosidad cinemática ν, m²/s	Número de Prandtl Pr
−150	2.866	983	0.01171	4.158×10^{-6}	8.636×10^{-6}	3.013×10^{-6}	0.7246
−100	2.038	966	0.01582	8.036×10^{-6}	1.189×10^{-5}	5.837×10^{-6}	0.7263
−50	1.582	999	0.01979	1.252×10^{-5}	1.474×10^{-5}	9.319×10^{-6}	0.7440
−40	1.514	1002	0.02057	1.356×10^{-5}	1.527×10^{-5}	1.008×10^{-5}	0.7436
−30	1.451	1004	0.02134	1.465×10^{-5}	1.579×10^{-5}	1.087×10^{-5}	0.7425
−20	1.394	1005	0.02211	1.578×10^{-5}	1.630×10^{-5}	1.169×10^{-5}	0.7408
−10	1.341	1006	0.02288	1.696×10^{-5}	1.680×10^{-5}	1.252×10^{-5}	0.7387
0	1.292	1006	0.02364	1.818×10^{-5}	1.729×10^{-5}	1.338×10^{-5}	0.7362
5	1.269	1006	0.02401	1.880×10^{-5}	1.754×10^{-5}	1.382×10^{-5}	0.7350
10	1.246	1006	0.02439	1.944×10^{-5}	1.778×10^{-5}	1.426×10^{-5}	0.7336
15	1.225	1007	0.02476	2.009×10^{-5}	1.802×10^{-5}	1.470×10^{-5}	0.7323
20	1.204	1007	0.02514	2.074×10^{-5}	1.825×10^{-5}	1.516×10^{-5}	0.7309
25	1.184	1007	0.02551	2.141×10^{-5}	1.849×10^{-5}	1.562×10^{-5}	0.7296
30	1.164	1007	0.02588	2.208×10^{-5}	1.872×10^{-5}	1.608×10^{-5}	0.7282
35	1.145	1007	0.02625	2.277×10^{-5}	1.895×10^{-5}	1.655×10^{-5}	0.7268
40	1.127	1007	0.02662	2.346×10^{-5}	1.918×10^{-5}	1.702×10^{-5}	0.7255
45	1.109	1007	0.02699	2.416×10^{-5}	1.941×10^{-5}	1.750×10^{-5}	0.7241
50	1.092	1007	0.02735	2.487×10^{-5}	1.963×10^{-5}	1.798×10^{-5}	0.7228
60	1.059	1007	0.02808	2.632×10^{-5}	2.008×10^{-5}	1.896×10^{-5}	0.7202
70	1.028	1007	0.02881	2.780×10^{-5}	2.052×10^{-5}	1.995×10^{-5}	0.7177
80	0.9994	1008	0.02953	2.931×10^{-5}	2.096×10^{-5}	2.097×10^{-5}	0.7154
90	0.9718	1008	0.03024	3.086×10^{-5}	2.139×10^{-5}	2.201×10^{-5}	0.7132
100	0.9458	1009	0.03095	3.243×10^{-5}	2.181×10^{-5}	2.306×10^{-5}	0.7111
120	0.8977	1011	0.03235	3.565×10^{-5}	2.264×10^{-5}	2.522×10^{-5}	0.7073
140	0.8542	1013	0.03374	3.898×10^{-5}	2.345×10^{-5}	2.745×10^{-5}	0.7041
160	0.8148	1016	0.03511	4.241×10^{-5}	2.420×10^{-5}	2.975×10^{-5}	0.7014
180	0.7788	1019	0.03646	4.593×10^{-5}	2.504×10^{-5}	3.212×10^{-5}	0.6992
200	0.7459	1023	0.03779	4.954×10^{-5}	2.577×10^{-5}	3.455×10^{-5}	0.6974
250	0.6746	1033	0.04104	5.890×10^{-5}	2.760×10^{-5}	4.091×10^{-5}	0.6946
300	0.6158	1044	0.04418	6.871×10^{-5}	2.934×10^{-5}	4.765×10^{-5}	0.6935
350	0.5664	1056	0.04721	7.892×10^{-5}	3.101×10^{-5}	5.475×10^{-5}	0.6937
400	0.5243	1069	0.05015	8.951×10^{-5}	3.261×10^{-5}	6.219×10^{-5}	0.6948
450	0.4880	1081	0.05298	1.004×10^{-4}	3.415×10^{-5}	6.997×10^{-5}	0.6965
500	0.4565	1093	0.05572	1.117×10^{-4}	3.563×10^{-5}	7.806×10^{-5}	0.6986
600	0.4042	1115	0.06093	1.352×10^{-4}	3.846×10^{-5}	9.515×10^{-5}	0.7037
700	0.3627	1135	0.06581	1.598×10^{-4}	4.111×10^{-5}	1.133×10^{-4}	0.7092
800	0.3289	1153	0.07037	1.855×10^{-4}	4.362×10^{-5}	1.326×10^{-4}	0.7149
900	0.3008	1169	0.07465	2.122×10^{-4}	4.600×10^{-5}	1.529×10^{-4}	0.7206
1000	0.2772	1184	0.07868	2.398×10^{-4}	4.826×10^{-5}	1.741×10^{-4}	0.7260
1500	0.1990	1234	0.09599	3.908×10^{-4}	5.817×10^{-5}	2.922×10^{-4}	0.7478
2000	0.1553	1264	0.11113	5.664×10^{-4}	6.630×10^{-5}	4.270×10^{-4}	0.7539

Nota: Para gases ideales, c_p, k, μ y Pr son independientes de la presión. Las propiedades ρ, ν y α a una presión P distinta a 1 atm se determinan cuando se multiplican los valores de ρ a la temperatura dada por P (en atm) y cuando se dividen ν y α entre P (en atm).

Fuente: Datos generados a partir del Software EES desarrollado por S. A. Klein y F. L. Alvarado. Fuentes originales: Keenan, Chao, Keyes, Gas Tables, Wiley, 198; and Thermophysical Properties of Matter, Vol. 3: Thermal Conductivity, Y. S. Touloukian, P. E. Liley, S. C. Saxena, Vol. 11: Viscosity, Y. S. Touloukian, S. C. Saxena, y P. Hestermans, IFI/Plenum, NY, 1970, ISBN 0-306067020-8.

Figure A1. Extracted from Çengel, Yunus A. y John M. Cimbala, “Mecanica de fluidos: Fundamentos y aplicaciones”, 1a edición, McGraw-Hill, 2006

APPENDIX 2: MATERIALS CORROSION

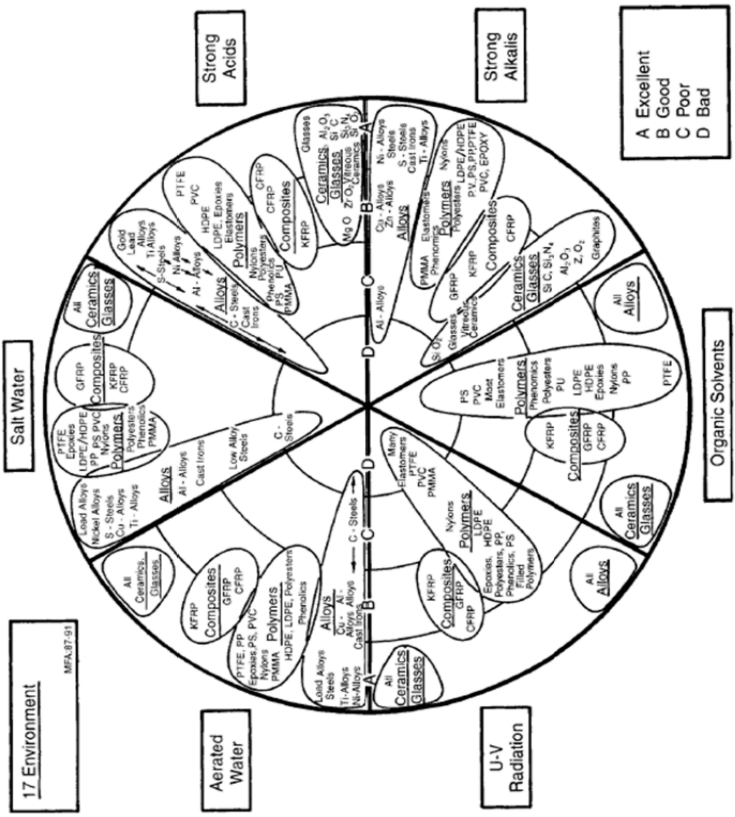

Figure A2. Extracted from Ashby, Michael F. "Materials Selection in Mechanical Design", 3rd Edition, Butterworth-Heinemann**,** 2005

APPENDIX 3: EXCEL WORKSHEET

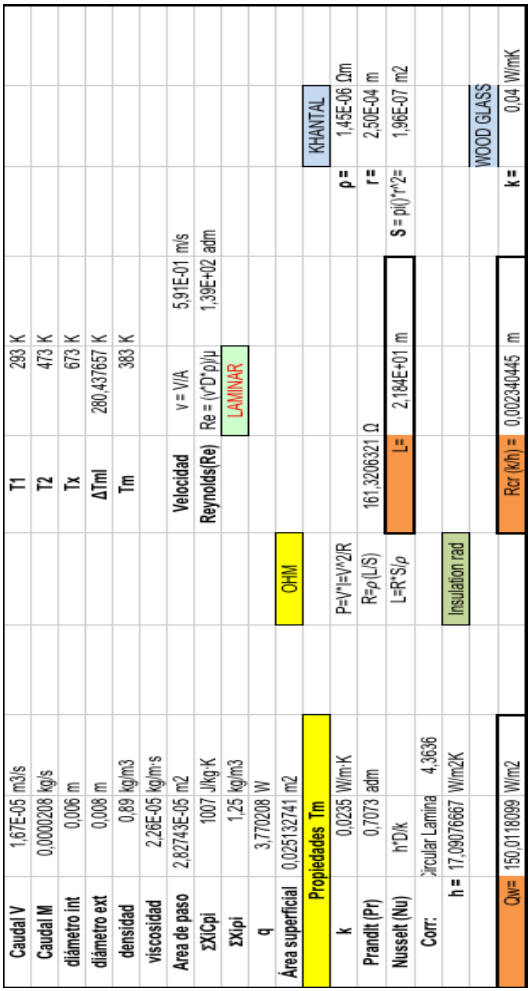

Caudal V	1,67E-05	m3/s		**T1**	293	K					
Caudal M	0,0000208	kg/s		**T2**	473	K					
diámetro int	0,006	m		**Tx**	673	K					
diámetro ext	0,008	m		**ΔTml**	280,437657	K					
densidad	0,89	kg/m3		**Tm**	383	K					
viscosidad	2,26E-05	kg/m·s									
Area de paso	2,82743E-05	m2		**Velocidad**	v = V/A	5,91E-01	m/s				
ΣXiCpi	1007	J/kg·K		**Reynolds(Re)**	Re = (v*D*p)/μ	1,39E+02	adm				
ΣXipi	1,25	kg/m3			LAMINAR						
q	3,770208	W									
Área superficial	0,025132741	m2		OHM						KHANTAL	
Propiedades Tm									**ρ =**	1,45E-06	Ωm
k	0,0235	W/m·K	P=V*I=I^2/R						**r =**	2,50E-04	m
Prandlt (Pr)	0,7073	adm	R=ρ(L/S)	161,3206321	Ω						
Nusselt (Nu)	h*D/k		L=R*S/ρ	**L=**	2,184E+01	m		**S = pi()*r^2=**	1,96E-07	m2	
Corr:	Circular Lamina	4,3636									
h =	17,09076667	W/m2K	Insulation rad								
										WOOD GLASS	
Qw=	150,0118099	W/m2		**Rcr (k/h) =**	0,002340445	m			**k =**	0,04	W/mK

Figure A3. Calculations for fluid mechanics and heat transfer